Heliyon 8 (2022) e08622

Contents lists available at ScienceDirect

Heliyon

journal homepage: www.cell.com/heliyon

Research article

Stem cell-derived exosomes and copper sulfide nanoparticles attenuate the progression of neurodegenerative disorders induced by cadmium in rats

Asmaa Magdy Zaazaa [a], Bosy Azmy Abd El-Motelp [a], Naglaa A. Ali [b,**], Ahmed M. Youssef [c], Mohamed Aly Sayed [d], Safaa H. Mohamed [b,*]

[a] Zoology Department, Faculty of Women for Arts, Science and Education, Ain Shams University, AsmaaFahmy Street Heliopolis, Cairo, Egypt
[b] Hormones Department, Research Division, National Research Centre, 33 El-Buhouth St., Dokki, Giza, 12622, Egypt
[c] Inorganic Chemistry Department, National Research Centre, 33 El-Buhouth St., Dokki, Giza, 12622, Egypt
[d] Department of Animal Reproduction and A. I., Veterinary Research Division, National Research Centre, 33 Bohouth St. Dokki, Cairo, Egypt

ARTICLE INFO

Keywords:
Stem cells
Exosomes
Cadmium
Nanotechnology
Neurological disorders

ABSTRACT

The goal of the current study was to investigate the therapeutic effects of exosomes derived from mesenchymal stem cells (MSCs-Exo) and copper sulfide nanoparticles (CuSNPs) as biomaterials in order to understand the mechanisms that contribute to overcoming cadmium (Cad) induced neurological disorders in rats. Animals were divided into five groups (n = 10): group 1 was served as a negative control and receive vehicle saline (Con), group 2 Positive control groups were received Cad as cadmium chloride at a dose of 20 mg/kg/day for six weeks (Cad group), group 3 was received Cad plus MSCs-Exo as a single dose of 100 μLi. v. (Cad + MSCs-Exo), group 4 was received Cad plus CuSNPs at a dose of 6.5 mg/kg orally (Cad + CuSNPs), group 5 was received Cad + MSCs-Exo + CuSNPs for six weeks. However, the activities of each acetylcholine (Ach), acetylcholinesterase (AchE), total antioxidant status (TAC) were measured. Also, the levels of ROS, nuclear factor kappa B (NF-κB), tumor necrosis factor-α (TNF-α), Brain brain-derived neurotrophic factor (BDNF) and nerve growth factor (NGF) were evaluated. Beneficial effects on the behavior of animals were observed after treatment with MSCs-Exo and CuSNPs. Furthermore, the administration of MSCs-Exo and CuSNPs have been improve the TAC, BDNF and NGF *via* ameliorating the oxidative stress and inflammatory markers. Moreover, Histopathological studies had shown that great development in the brain of Cad rats treated with MSCs-Exo and CuSNPs. In conclusion, this study offers an overview of innovative stem cell therapy techniques and how to integrate them with nanotechnology to boost therapeutic performance.

1. Introduction

Cadmium (Cad) is one of the most toxic ingredients in the environment owing to its wide range of organ toxicity and long elimination half-life of 10–30 years [1]. It is associated with a more pronounced death of cholinergic neurons from the basal forebrain mediated, in part, by an increase in amyloid plaques (Aβ) and phosphorylated Tau protein. This may explain the effects of cadmium on memory processes and learning [2]. Exposure to Cad, which is a persistent neurotoxic environmental pollutant [3], has been associated with numerous human pathologies, including kidney dysfunction, osteoporosis, birth defects, respiratory ailments, and neurodegenerative diseases [4].

Mesenchymal stem cells (MSCs) have been investigated as a delivery tool to straightforwardly target therapies to the brain for the treatment of a variety of brain diseases. They are clinically useful owing to their capacity for self-renewal, immunomodulatory properties, and tissue regenerative potential [5]. MSCs are a versatile class of multipotent adult stem cells found in various tissues throughout the body, with the most abundant and accessible in the bone marrow, adipose, and placental tissues. These cells generate the various connective tissues of the body and can generate other cell types, including myocytes and functional neurons [6]. Aside from their role in repopulation, MSCs are uniquely capable of homing to areas of inflammation to function as anti-inflammatory cells as well as exhibiting neuro protective effects [7].

* Corresponding author.
** Corresponding author.
E-mail addresses: almardeyah@hotmail.com (N.A. Ali), rise_sun_1982@hotmail.com (S.H. Mohamed).

https://doi.org/10.1016/j.heliyon.2021.e08622
Received 20 August 2021; Received in revised form 5 November 2021; Accepted 14 December 2021

Exosomes (Exo) are extracellular vesicles with a diameter of 40–100 nm and a density of 1.13–1.19 g/mL; they contain proteins, mRNA, miRNAs, and DNA. Exosomes change the biochemical features of recipient cells through biomolecule delivery and play a role in cellular communication. These vesicles are produced from body fluids and different cell types like MSCs [8].

Among the different classes of materials suitable for drug delivery, biodegradable polymer nanoparticles (NPs) have attracted significant attention because of their safety as well as mechanical and optical properties [9]. Owing to their small size, NPs can readily enter the body through various routes, cross the blood–brain barrier, and remain in the central nervous system for long periods of time. Therefore, it is important to thoroughly investigate the pathobiological changes in the nervous system in response to NPs exposure [10].

Metallic NPs, particularly composed of copper sulfide nanoparticles (CuSNPs), are involved in the vital functions in the body, such as growth, digestion, hematopoiesis, and immunity [11]. CuSNPs have been used in numerous applications, including bacterial infection, anti-tumor therapy, lubricants for metallic coating, additives for livestock and poultry feed, and osteoporosis treatment [12]. In this study, we explored the mechanisms through which the biomaterials, MSC-exosomes (MSC-Exo) and CuSNPs, modulate the cholinergic system, behavioral deficits, oxidative stress, and neuroinflammation and enhance neurologic growth factors to ameliorate cadmium-induced neurotoxicity in rats.

2. Materials and methods

2.1. Chemicals and reagents

Cadmium was purchased from Sigma-Aldrich Chemicals Co. All the other reagents, solvents, and chemicals used for analysis met the quality criteria in accordance with the international standards.

Copper (II) sulfate pentahydrate from Aldrich Chemical Co. Ltd, Sodium sulfide nanohydrate from Riedel-de Haen.

2.1.1. Preparation and isolation of bone marrow-derived mesenchymal stem cells (MSCs)

Bone marrow was harvested by flushing the tibiae and femurs of 6-week-old male Wistar rats with phosphate-buffered saline (PBS). Bone marrow cells were seeded in Dulbecco's Modified Eagle's Medium supplemented with 10% fetal bovine serum. Nucleated cells were isolated using a density gradient and resuspended in a complete culture medium supplemented with 1% penicillin–streptomycin. Cells were incubated at 37 °C in a 5% humidified CO_2 incubator for 12–14 days as a primary culture or upon formation of large colonies. When large colonies developed (80%–90% confluence), the plates were washed twice with PBS (pH 7), and the cells were trypsinized with 0.25% trypsin in 1-mM ethylenediaminetetraacetic acid for 5 min at 37 °C. After centrifugation at 3000 rpm for 10 min, the cells were resuspended in serum-supplemented medium and seeded into 50-cm^2 culture flasks. The resulting cultures were referred to as first-passage cultures [13]. Cells were identified as MSCs by their fusiform shape morphology and adherence and *via* fluorescence-activated cell sorting with the detection of CD29+, CD90+, and CD45− specific to MSCs [14].

2.1.2. Characterization of the surface markers of MSCs via flow cytometry

Cells were resuspended in wash buffer after a quick centrifugation (BD Biosciences, Germany). The cell suspension (300 μL) was incubated with antibodies against CD29, CD34, and CD90 conjugated with allophycocyanin (APC), cyanine 5 (CY5), phycoerythrin (PE), and fluorescein isothiocyanate (FITC) dyes, respectively, for 45 min at room temperature. Flow cytometry was performed using FACS Calibur (BD Biosciences, Germany), and the Cell Quest software was used for analysis.

2.1.3. Isolation and characterization of rat MSC-Exo

Exosomes were derived from the supernatants of third passage MSCs (5×10^6 cells/mL) that were cultivated in serum-free RPMI supplemented with 0.5% bovine serum albumin (BSA) (Sigma-Aldrich). To eliminate debris, the cell-free supernatant was centrifuged at 2000g for 20 min, followed by centrifugation at 100,000g (Beckman Coulter Optima L-90K ultracentrifuge) for 1 h at 4 °C. The collected cell pellet was subsequently washed with serum-free medium containing 25-mM HEPES (Sigma-Aldrich) and subjected to a second ultra-centrifugation under the same conditions. The quantification of protein content was performed using the Bradford protein assay (Bio-Rad, Hercules, California, USA). The sanitized extracellular exosomes (Exo) were then cultured overnight in the media used for Exo gathering. Flow cytometry analysis was conducted using FITC-conjugated antibodies, namely, CD83 (Miltenyi Biotec, Bergisch, Germany) and CD73 (Becton Dickinson, New Jersey, USA), whereas FITC mouse non-immune isotypic IgG (Dako Cytomation, Glostrup, Denmark) was used as a control [15].

2.1.4. Tracking of MSC-Exo

The purified MSC-Exo cells were labeled using a PKH67 kit (Sigma-Aldrich) according to the procedure reported by Bang et al. [15]. Briefly, exosomes diluted in PBS were added to 0.5 mL of Diluent C. At the same time, 4 mL of the PKH26/PKH67 dyes were added to 0.5 mL of Diluent C and incubated for 4 min at room temperature with the exosome solution. To bind excess dye, 2mL of 0.5% BSA/PBS was added. The labeled exosomes were washed at 100,000× g for 1 h, and the exosome pellet was resuspended with PBS and used for uptake experiments.

2.1.5. Characterization of nanomaterials

Experiments were conducted with different molar ratios of the compositions of Cu^{2+} and S^{2-} at a temperature of 220 °C. The experimental details were as follows: $CuSO_4.5H_2O$ powder and $Na_2S.7H_2O$ powder were dissolved separately in deionized water and stirred at room temperature for 30 min. A Na_2S solution was added dropwise to the CuSO4 solution while stirring. Copper and sulfur at a 1:1 M ratio were used for the synthesis. The chemical reactions may be described as follows [16]:

$$CuSO_4 \leftrightarrow Cu^{2+} + SO_4^{2-} \quad (1)$$

$$Cu^{2+} + Na_2S \leftrightarrow CuS + 2Na^{+} \quad (2)$$

The resulting white gels were placed into a Teflon-lined stainless-steel autoclave and filled with the mixture to 50% of its volume. The closed chamber was placed inside a box furnace (Mermert-500) at a temperature of 220 °C for 12 h and then allowed to cool down to room temperature. The solution containing the product was centrifuged, the supernatant was decanted, and the pellet was washed with double-distilled water. The washing procedure was repeated 10 times to remove impurities in the sample. The final white product was air-dried at 60 °C for 12 h.

2.1.6. Animal protocol and dietary treatments

All experiments involving animals and tissue samples were conducted in accordance with the Guide for the Care and Use of Laboratory Animals of the US National Institutes of Health. This study was approved by the Ethical Committee on Animal Experimentation, National Research Center, Egypt, and conducted in the Hormones lab, Medical Research Division, National Research Center, Giza, Egypt.

A total of 50 12-week-old male Wistar strain rats, weighing 150–200 g, were obtained from the Animal House Colony of the National Research Center. They were housed in plastic cages at a room temperature of 25 °C and humidity of 55% under a 12-h dark/light cycle. All animals were maintained under laboratory conditions for at least 2 weeks prior to the experiment and under the same conditions during the experiment.

One week before the start of the experiment, the rats were acclimatized. The animals were randomly divided into five experimental groups (10 rats/group) according to the following experimental protocol: **Group**

(1), negative control group (Con): the rats received the vehicle (saline) in which the drugs are dissolved in the same manner as the treated groups; **Group (2)**, positive control group (Cad): the rats received cadmium chloride at a dose of 20 mg/kg/day dissolved in 2mL of saline daily through a feeding tube for 6 weeks [17]; **Group (3)** (Cad + MSC-Exo): the rats received cadmium chloride at a dose of 20 mg/kg/day dissolved in 2mL of saline daily through a feeding tube for 6 weeks, followed by IV injection of a single dose of 100 μL of the respective exosome within 1 h after delivery [18];**Group (4)** (Cad + CuSNPs): the rats received cadmium chloride at a dose of 20 mg/kg/day dissolved in 2mL of saline daily through a feeding tube for 6 weeks and then administered a dose of CuSNPs (100 nm and 10 wide and 10 nm thickness) at a dose of 6.5 mg/kg orally [19] for 30 consecutive days; and **Group (5)** (Cad + MSC-Exo + CuSNPs): the rats received cadmium chloride at a dose of 20 mg/kg/day dissolved in 2mL of saline daily through a feeding tube for 6 weeks and then treated with both MSC-Exo and CuSNPs as described above.

2.1.7. Behavioral assessment

2.1.7.1. Forced swimming test (FST). In a transparent plastic cylinder (diameter: 40 cm, height: 60 cm), each rat was positioned individually and in full water to a height of 40 cm. The rats were forced to swim for 5 min. During the last 3 min, the time of immobility was registered. Immobility was characterized by stopping, struggling, and floating on the water surface. The test was video-recorded and analyzed. Each time, the water was replaced, and the temperature was maintained at 26 °C [20].

2.1.8. Sample collection

After 4 weeks of exosome and CuSNP administration, the rats were fasted overnight, then humanely euthanized *via* exsanguination under sodium pentobarbital anesthesia. The brains were excised immediately, and each was divided into two halves: one half was immediately homogenized to yield a 10% (w/v) homogenate in ice-cold medium containing 50-mM Tris-HCl and 300-mM sucrose (pH 7.4) [21]. The homogenate was centrifuged at 1800× g for 10 min at 4 °C. For the biochemical assays, the supernatant (10%) was isolated. The other half of each brain was fixed in formalin buffer (10%) for histopathological examination.

2.1.9. Biochemical analyses

Quantitative estimation of total protein levels in brain homogenates was performed according to the method described by Lowry et al. [22].

2.1.9.1. Measurement of cholinergic function. The brain acetylcholine (Ach) content was measured *via* enzyme-linked immunosorbent assay (ELISA) using a choline/acetylcholine assay kit purchased from BioVision Research Product Co. (Linda Vista Avenue, USA) according to the method described by Ostwald et al. [23]. The level of brain acetylcholinesterase (AChE) was calculated colorimetrically using the method indicated in the acetylcholinesterase assay kit purchased from Centronic GmbH Am Kleinfeld 11,85456 (Wartenberg, Germany) and previously described by Henry [24].

2.1.9.2. Oxidative stress and antioxidant content measurements. The generation of reactive oxygen species (ROS) in the brain tissue was measured using the ROS Assay Kit (Cell Biolabs Inc., San Diego CA, USA) following the manufacturer's protocol. In accordance with the method described by Koracevic et al. [25], the total antioxidant capacity (TAC) was measured colorimetrically using a kit purchased from Biodiagnostic Co., Egypt.

2.1.9.3. Measurement of inflammatory status. The levels of brain nuclear factor kappa B (NF-κB) were measured *via* ELISA using a kit purchased from Glory Science Co., USA, according to the method described by Adams [26]. The levels of brain tumor necrosis factor-α (TNF-α) were also measured *via* ELISA using a kit purchased from AviBion Co., USA, according to the method described by Intiso et al. [27].

2.1.9.4. Measurement of growth factors. The levels of brain-derived neurotrophic factor (BDNF) were detected *via* ELISA using a kit purchased from Ray Biotech, Inc., USA, according to the method described by Barde [28]. The brain nerve growth factor (NGF) content was measured using an ELISA kit (Chemicon, Temecula, CA, USA) according to the manufacturer's protocol.

2.1.9.5. Histopathological evaluation. After fixing the brain specimens in formal saline (10%) for 24 h and washing with tap water, the samples were subjected to serial dilutions of alcohol (methyl, ethyl, and absolute ethyl) for dehydration. Subsequently, the brain samples were cleaned of xylene and placed in paraffin wax at 56 °C for 24 h in a hot air oven. Paraffin-embedded tissue blocks were prepared *via* sectioning at 4μmusing a sledge microtome. The resulting tissue sections were transferred onto glass slides, deparaffinized, and stained with hematoxylin and eosin (H&E) [29]. The slides were viewed using an Olympus CH (Japan) light microscope. The image was captured using a digital camera (Sony Dscow 3, Japan), and photomicrograph calibration was performed using the Image J software [30].

2.2. Statistical analysis

The data are expressed as mean ± standard error (SE). The Statistical Package for the Social Sciences software, version19.0, was used to compare the two groups. Differences were considered significant at P-values ˂0.05. The percentage difference representing the percentage variation with respect to the corresponding control group [31] was calculated using the following formula:

$$\% \text{ Difference} = [(\text{Treated value} - \text{control value})/\text{control value}] \times 100$$

3. Results

3.1. Cell surface marker expression analysis and characterization via flow cytometry

Flow cytometry analysis revealed the immunophenotype of MSCs. MSCs were negative for the hematopoietic marker CD45 (Figure 1A) and strongly positive for MSC-specific markers, including CD29 (Figure 1B) and CD90 (Figure 1C).

3.1.1. Characterization of rat MSC-Exosomes via flow cytometry and tracking of the exosomes

The immunophenotype of MSC-Exo cells was evaluated *via* flow cytometry. MSC-Exo cells were negative for the hematopoietic marker CD34 (A), whereas they were strongly positive for the Exo-specific markers, namely, CD73 (Figure 2B) and CD83 (Figure 2C). MSC-Exo cells were labeled with PKH26 to track their engraftment in the brain tissue (Figure 3A and B).

3.1.2. Characterization of the nanomaterial

Figure 4 presents the XRD patterns of the sample prepared using a hydrothermal method. According to the JCPDS file no. 78–0876 (a = b = 3.7918 Å and c = 16.3660 Å) [32], the XRD pattern of the CuS sample demonstrated a hexagonal structure. No impurities, such as CuO or other nonstoichiometric CuS, were detected. The XRD peaks were quite broad, indicating that the nanocrystalline structure resulted from the prepared sample.

The morphology of pure CuS nanopowder, which was prepared using a hydrothermal method and heated to 60 °C, was analyzed *via* transmission electron microscopy, as presented in Figure 5. Very fine nanowires agglomerated together were observed. Hexanano plates were observed in the sample, which were 100-nm wide and 10-nm thick. The

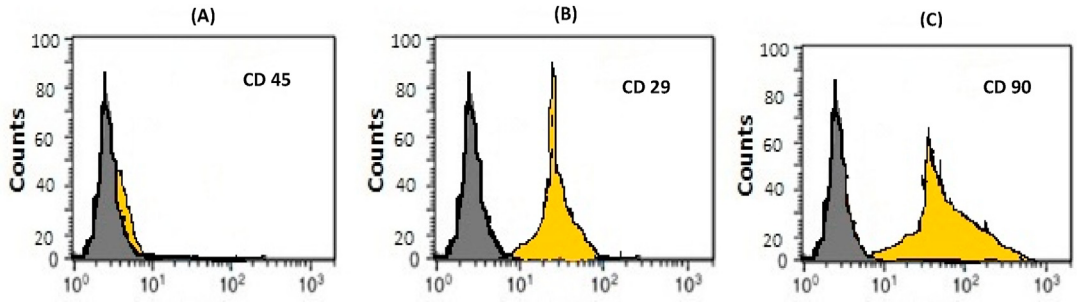

Figure 1. Flow cytometry analysis of the immunophenotype of MSCs. MSCs were negative for CD45 (A) and strongly positive for CD29 (B) and CD90 (C). The yellow histograms indicate the antibody-labeled cells, whereas the gray histogram indicates the profile of the isotype control.

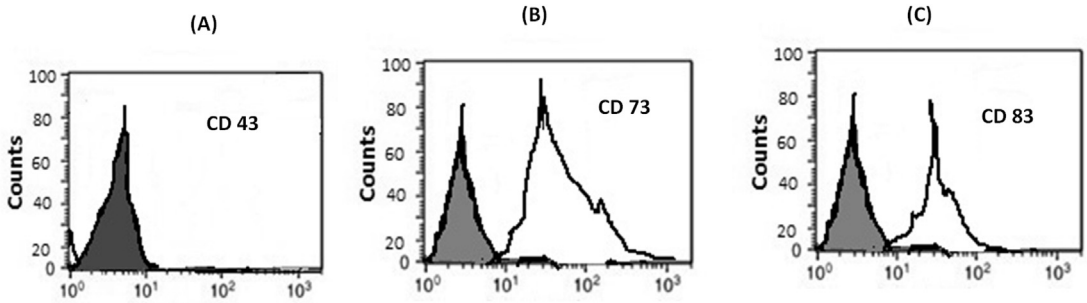

Figure 2. Immunophenotype of MSC-Exo cells as determined via flow cytometry. MSC-Exo cells were negative for the hematopoietic marker CD34 (A), whereas they were strongly positive for the Exo-specific markers, namely, CD73 (B) and CD83 (C). The white histograms indicate the antibody-labeled cells, whereas the gray histogram indicates the profile of the isotype control.

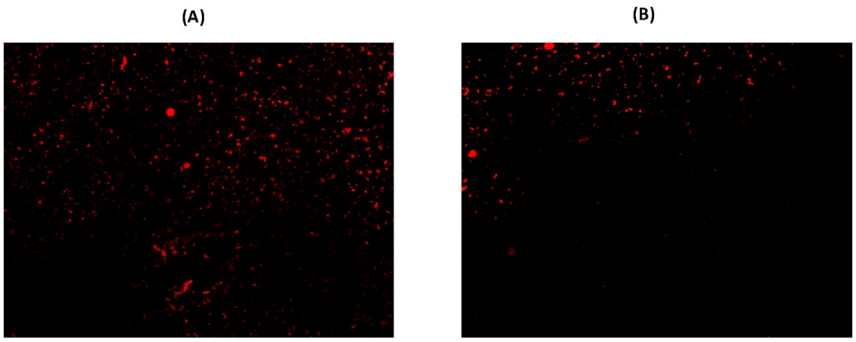

Figure 3. Cad + MSC-Exo group showing the PKH26-labeled injected exosomes engrafted in the brain tissue (A) and the Cad + MSC-Exo + CuSNP group showing the PKH26-labeled injected stem cells engrafted in the brain tissue (B).

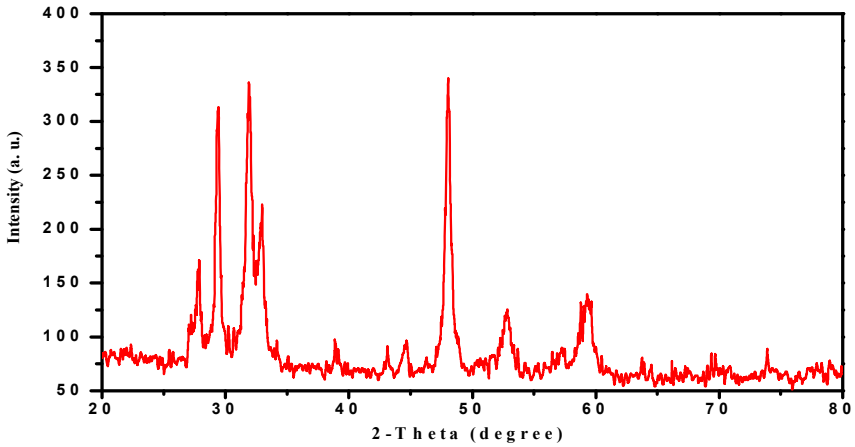

Figure 4. XRD patterns of CuS nanostructures, with Cu^{2+}/S^{2-} having a molar ratio of 1:1.

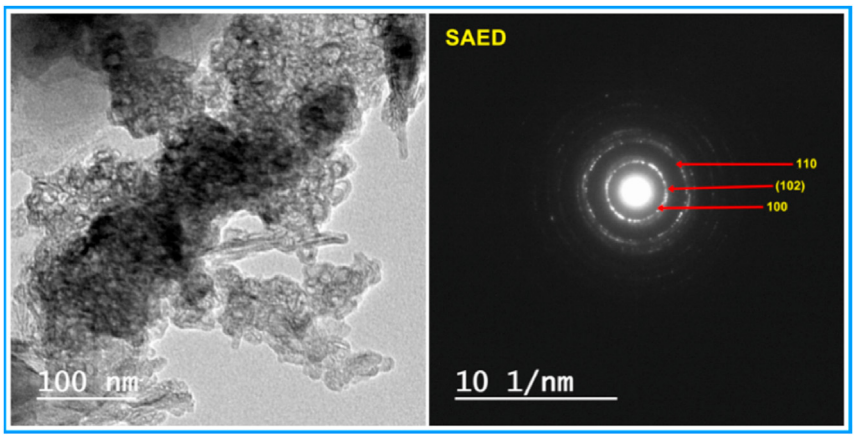

Figure 5. TEM and SAED image of CuS nanopowder prepared using Cu^{2+}/S^{2-}at a molar ratio of 1:1.

selected area electron diffraction (SAED) patterns appeared as randomly bright spots, indicating that the sample exhibited good crystallinity with different orientations. The strong diffraction rings were interpreted and specified as the (100), (102), and (110) planes for hexagonal CuS and were readily observed and consistent with the XRD results.

Figure 6 presents typical EDAX patterns and details of the relative analysis of this sample. The spectrum shows the expected elements. The elemental analysis was only conducted for (CuS) Cu and S, and the average atomic percentage was 50.34:49.66. The quantitative analysis of the Cu/S atomic ratio was 50.34:49.66, which was close to 1:1 and in accordance with its chemical formula [33]. Table 1. Showed EDX spectrum of CuS powder synthesized at 60 °C.

Table 1. EDX spectrum of CuS powder synthesized at 60 °C.

Element	Weight %	Atomic %	Net Int	Error %
S K	33.24	49.66	349.84	5.31
CuK	66.76	50.34	173.19	3.53

3.2. Behavioral assessment

Table 2 presents the Cad-induced behavioral disorder in male rats in the FST, which is evidenced by a significant increase in immobility compared with the control rats ($P < 0.05$). In contrast, the Cad rats that received MSC-Exo and CuSNPs exhibited a significant reduction in immobility duration compared with the Cad rats ($P < 0.05$), suggesting that MSC-Exo and CuSNPs may function as neuroprotective agents.

3.2.1. Effect of MSC-Exo and CuSNPs on the cholinergic function in the brain tissue of cadmium-treated rats

Figure 7 presents the expected toxicity resulting from Cad treatment of rats. Compared with the negative control group, there was a significant increase in AChE activity ($P < 0.05$) associated with a significant reduction ofthe levels of ACh and AChT ($P < 0.05$) in the Cad-treated group. Cad rats treated with MSC-Exo and CuSNPs or both exhibited a significant improvement in all cholinergic functions in the brain tissue, particularly in the MSC-Exo + CuSNP group, which confirmed beneficial effects compared with the untreated Cad rats.

3.2.2. Effect of MSC-Exo and CuSNPs on the oxidative stress and antioxidant content of the brain tissue from cadmium-treated rats

The ROS levels were significantly increased ($P < 0.05$) in the Cad group compared with the normal control group. However, the level of TAC showed a significant ($P < 0.05$) reduction compared with the negative control. Administration of MSC-Exo and CuSNPs caused significant changes in the tissue levels of ROS and TAC compared with the Cad group. Furthermore, the administration of MSC-Exo + CuSNPs significantly ($P < 0.05$) reduced the tissue levels of ROS and significantly ($P < 0.05$) elevated the tissue levels of TACcompared with that of the Cad-treated group (Figure 8).

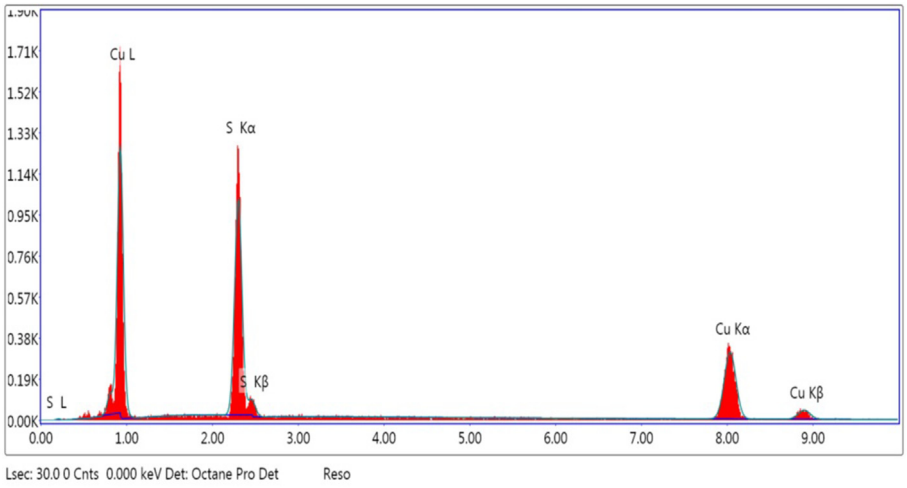

Figure 6. Typical EDAX patterns.

Table 2. Effect of treatment with MSC-Exo and CuSNPs on the immobility time (s) of cadmium chloride-treated rats in the forced swimming test (data are expressed as mean ± SE for 10 rats/group).

Parameter			
Groups	Immobility time (s)		
	Zero time	After 45 days of cadmium chloride administration	After 75 days of cadmium chloride administration
Con	43.00 ± 6.28	45.32 ± 5.92	46.26 ± 5.42
Cad	45.00 ± 7.74	120.37 ± 10.82[a]	129.73 ± 10.14[a]
Cad + MSC-Exo	44.00 ± 6.22	125.36 ± 8.63[a]	78.82 ± 7.13[b,c]
Cad + CuSNPs	41.00 ± 5.30	124.52 ± 9.12[a]	83.75 ± 8.42[b,c]
Cad + MSC-Exo + CuSNPs	42.00 ± 4.12	121.70 ± 10.64[a]	62.81 ± 5.34[b]

[a] $P < 0.05$ vs. the negative control group.
[b] $P < 0.05$ vs. the Cad group.
[c] $P < 0.05$ vs. Cad + MSC-Exo + CuSNP-treated group.

3.2.3. Effect of MSC-Exo and CuSNPs on the inflammatory markers in the brain tissue of cadmium-treated rats

As can be seen from Figure 9, the levels of TNF-α and NF-κB of Cad rats were significantly increased compared with that in the normal control rats. The levels were significantly ($P < 0.05$) decreased in all other groups after treatment with MSC-Exo and CuSNPs. Furthermore, a significant reduction ($P < 0.05$) in the levels of TNF-α and NF-κB were detected in the brain tissue of rats treated with MSC-Exo + CuSNPs.

3.2.4. Effect of MSC-Exo and CuSNPs on the growth factors in the brain tissue of the cadmium-treated rats

Figure 10 demonstrates that the brain levels of NGF and BDNF were significantly downregulated ($P < 0.05$) after Cad treatment compared with the normal control group. The administration of MSC-Exo and CuSNPs or MSC-Exo + CuSNPs significantly upregulated ($P < 0.05$) these levels compared with the Cad group.

3.3. Histopathological investigation

Histopathological examination of the brains of control rats revealed a normal histologic structure (Figure 11). Examination of the H&E-stained sections prepared from the cadmium-treated group revealed severe pathological lesions, whereas most sections demonstrated multiple extracellular vacuoles associated with peri neuronal vacuolations (Figure 12). Most of the examined neurons exhibited vacuolar degenerative changes, and these vacuoles were variable in size and associated with severe congestion of the meningeal blood vessels (Figure 13). Pyramidal cells were atrophied, showing necrosis, and appearing irregular in shape with darkly staining nuclei. Some sections demonstrated multifocal neuronophagia and focal gliosis (Figures 12 and 13).

Histopathological examination of the specimens obtained from rats treated with cadmium concomitantly with MSC-Exorevealed a slight

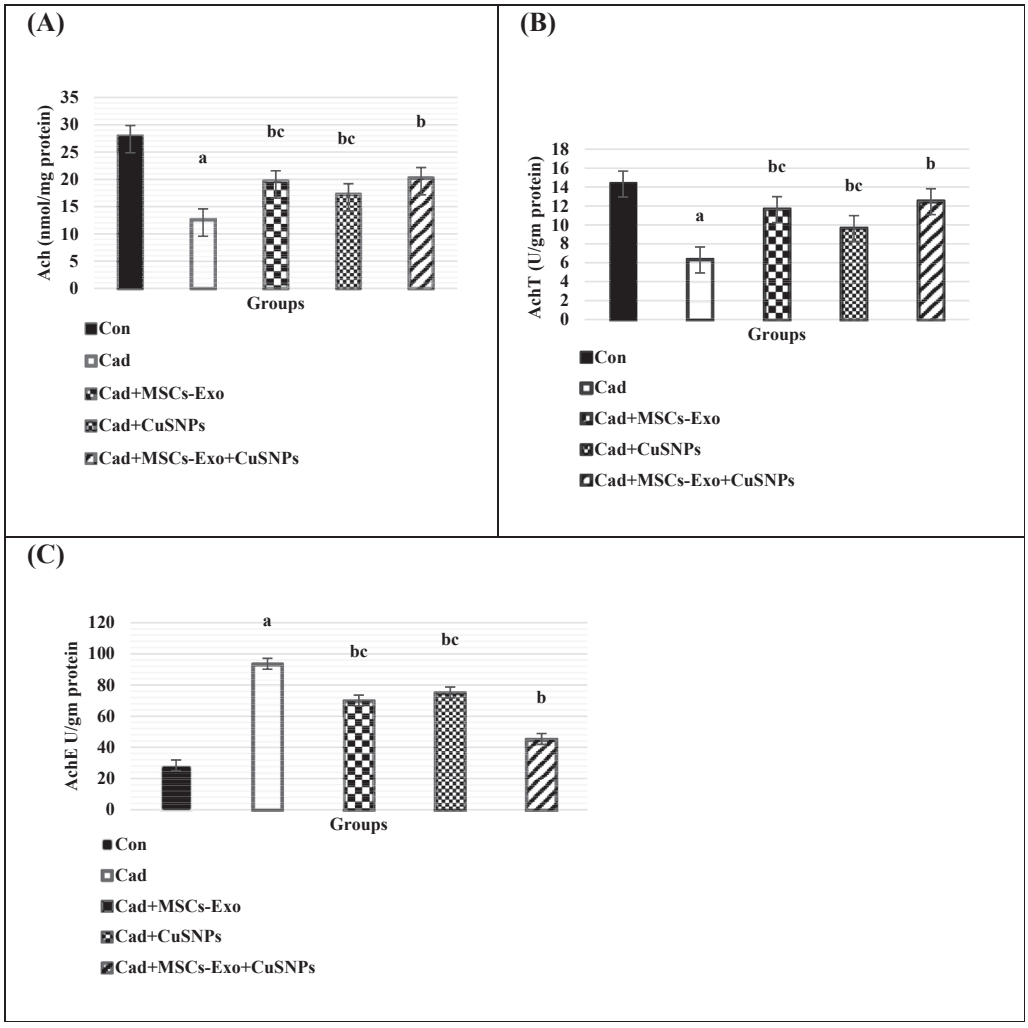

Figure 7. Effects of MSC-Exo and/or CuSNPs on the cholinergic function in the brain tissue of Cad-treated rats. (A) The level of ACh, (B) the activity of AChT, and (C) the activity of AChE were determined in the brain tissue homogenates of the Con group, Cad-treated group, Cad + MSC-Exo-treated group, Cad + CuSNP-treated group, and Cad + MSC-Exo + CuSNP-treated group. Data are expressed as mean ± SE. (a) Significant difference relative to the Con group; (b) significant difference relative to the Cad group, (c) significant difference relative to the Cad + MSC-Exo + CuSNP-treated group, $p < 0.05$ ($n = 10$).

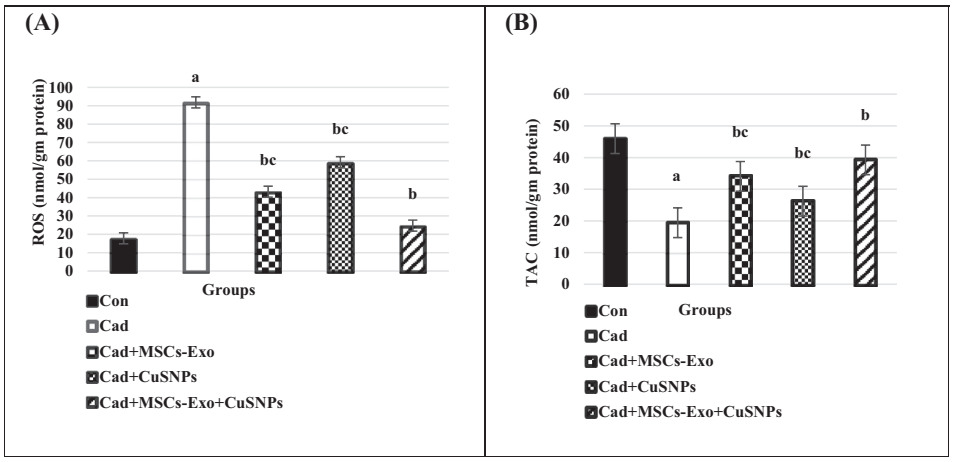

Figure 8. Effects of MSC-Exo and/or CuSNPs on the oxidative stress and antioxidant content inthe brain tissue of cadmium-treated rats. (A) The level of ROS and (B) the activity of TAC was determined in the brain tissue homogenates of the Con group, Cad-treated group, Cad + MSC-Exo-treated group, Cad + CuSNP-treated group, and Cad + MSC-Exo + CuSNP-treated group. Data are expressed as mean ± SE. (a) Significant difference relative to the Con group; (b) significant difference relative to the Cad group, (c) significant difference relative to the Cad + MSC-Exo + CuSNP-treated group, $p < 0.05$ ($n = 10$).

improvement in the nerve cells (Figure 14). Co-treatment with CuSNPs for 1 month showed improvement in many sections of the nerve cells. The sections revealed mildly congested blood vessels and mild vacuolar degenerative changes (Figure 15), whereas treatment with cadmium, MSC-Exo, and CuSNPs demonstrated a significant improvement in the pathological profile, showing only mild vacuolar degeneration (Figure 16).

4. Discussion

Human insinuation to Cad through tobacco smoking, mining waste, fertilizers, and sewage contamination thusly, reaches humans *via* nutrient intake [34]. A diversity of events has been embroiled in the pathophysiology of Cad-induced neurotoxicity and progression of the central nervous system (CNS).

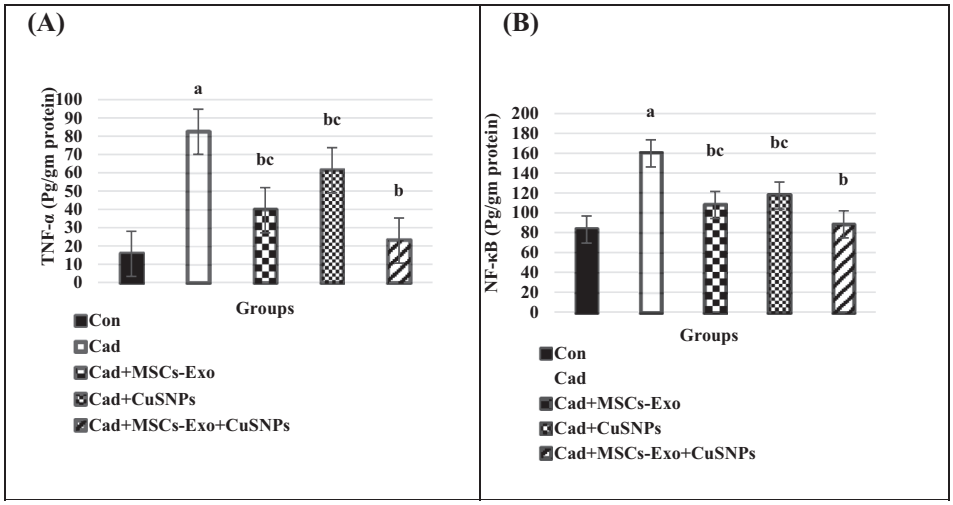

Figure 9. Effects of MSC-Exo and/or CuSNPs on the inflammatory markers in the brain tissue of cadmium-treated rats. (A) The level of TNF-α and (B) the level of NF-κB were determined in the brain tissue homogenates of the Con group, Cad-treated group, Cad + MSC-Exo-treated group, Cad + CuSNP-treated group, and Cad + MSC-Exo + CuSNP-treated group. Data are expressed as mean ± SE. (a) Significant difference relative to the Con group; (b) significant difference relative to the Cad group, (c) significant difference relative to the Cad + MSC-Exo + CuSNP-treated group, $P < 0.05$ ($n = 10$).

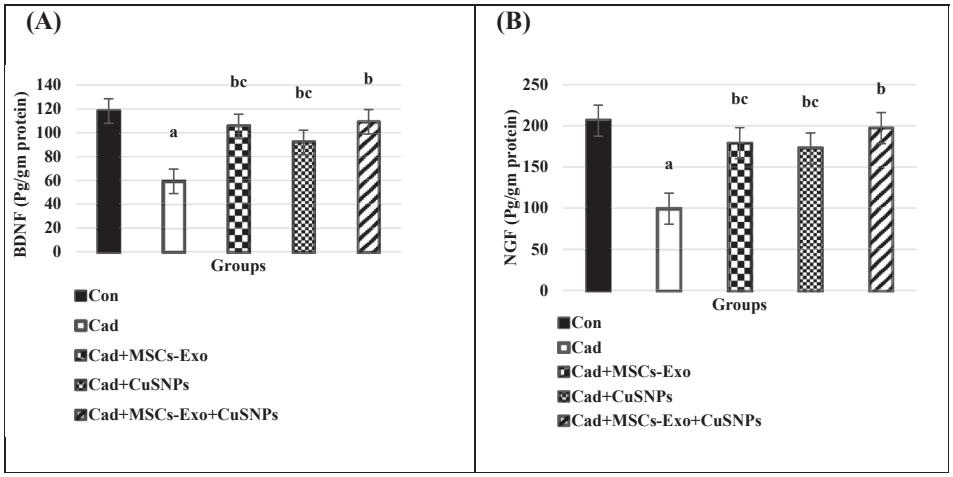

Figure 10. Effects of MSC-Exo and/or CuSNPs on the growth factors in the brain tissue of Cad-treated rats. (A) The level of BDNF and (B) the level of NGF were measured in the brain tissue homogenates of the Con group, Cad-treated group, Cad + MSC-Exo-treated group, Cad + CuSNP-treated group, and Cad + MSC-Exo + CuSNP-treated group. Data are expressed as mean ± SE. (a) Significant difference relative to the Con group; (b) significant difference relative to the Cad group, (c) significant difference relative to the Cad + MSC-Exo + CuSNP-treated group, $P < 0.05$ ($n = 10$).

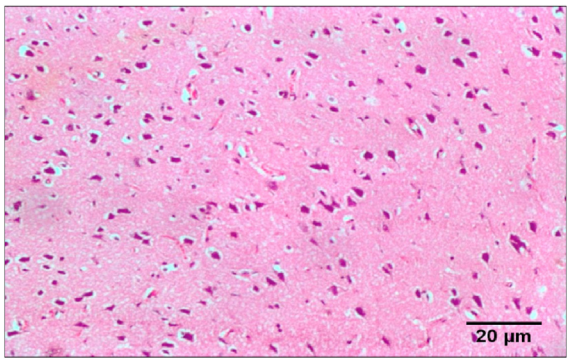

Figure 11. Photomicrograph of the brain of a control rat showing a normal histologic structure (H&E scale bar 20 µm).

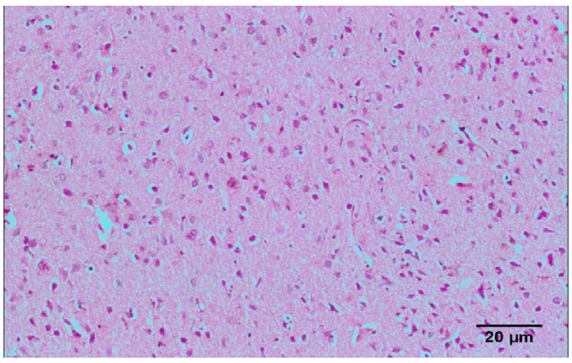

Figure 14. Photomicrograph of a section in the brain of a Cad + MSC-Exo-treated rat showing mild vacuolar degeneration (H&E scale bar 20 µm).

Our study demonstrated that Cad exposure was significantly and positively correlated with memory deficit, anxiogenic and depressive-like behaviors, and impairment in the FST. Cad is regarded as a potential neurotoxicant with a long biological half-life and the ability to partially cross the placenta and blood–brain barrier [35]. Moreover, Cad can cause oxidative stress and interfere with neuronal differentiation and neurotransmitters [36]. Therefore, continuous exposure, even at low levels, may lead to adverse neurobehavioral effects.

The present study demonstrated a significant decrease in the immobility time in the FST of the Cad group treated with MSC-Exo and CuSNPs or both compared with the Cad group. This finding may result from the MSC-Exo and CuSNPs acting as antidepressant-like agents. A study by Wang et al. [37] demonstrated that MSC-Exo significantly diminished the ROS production and apoptosis in cardiac stem cells (CSC) subjected to oxidative stress injury. Similarly, it is known that MSC-Exo increases retinal ganglion cell survival through miRNA-dependent mechanisms in traumatic ocular and degenerative diseases [38]. The positive function of MSC-Exo during cell progression is consistent with that of previous studies and could be responsible for the behavioral changes and protective activity toward depressive behavior. Otherwise, NPs could transform the microglial polarization state from a pro-inflammatory phenotype to an anti-inflammatory phenotype by scavenging ROS triggered by stress stimuli in the microglial cells [39]. This is a proposed mechanism through which CuSNPs could improve the immobility time in the FST.

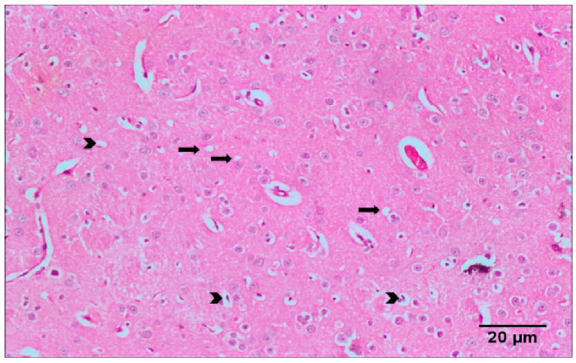

Figure 12. Photomicrograph of a section in the brain of a Cad-treated rat showing extracellular vacuoles (arrow) associated with perineuronal vacuolations (arrowhead) (H&E scale bar 20 µm).

The present study demonstrated a significant increase in the AChE activities correlated with a significant reduction in ACh and AChTin the Cad-treated group compared with the control group. These results may be due to the increased accumulation of Cad in the brain tissue and its ability to enter the brain parenchyma and neurons, causing neurological alterations and leading to decreasing serotonin and acetylcholine levels [40]. Our findings are in agreement with those of Mendez-Armenta and Rios [41], who reported that Cad expresses neurotoxic effects on the animal brain, disrupting synaptic neurotransmission balance (excitation/inhibition) and the release of acetylcholine by interfering with calcium metabolism.

We also observed that treatment of rats with MSC-Exo, CuSNPs, or both ameliorated the levels of AChE, ACh, and AChT compared with the Cad-treated group. This may occur because MSC-Exo and CuSNPs can differentiate neuronal and glial fates [42]. Consistent with our results, Snyder [43] found that treatment with stem cells can enhance neurogenesis in the models of degenerative diseases. Furthermore, the antioxidant properties of CuSNPs are similar to Cu and carbon-coated copper (Cu–C) NP suspensions, which contribute to the reduction of the AChE

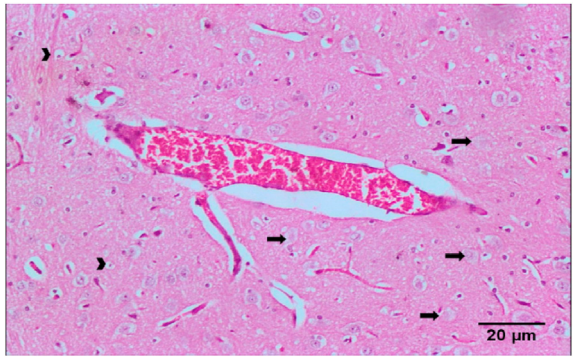

Figure 13. Photomicrograph of a section in the cerebral cortex of a Cad-treated rat showing severe meningeal vascular congestion associated with neuronal degeneration (arrows) and perineuronal vacuolations (arrowhead) (H&E scale bar 20 µm).

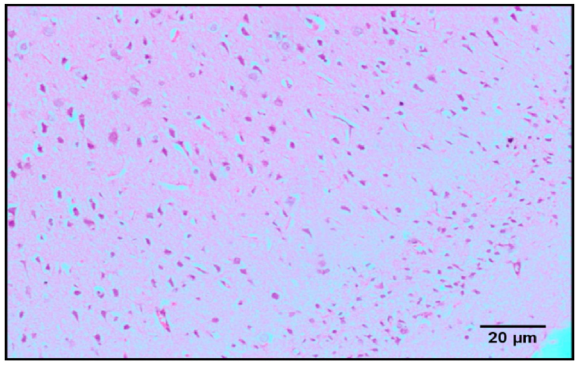

Figure 15. Photomicrograph of a section in the brain of a Cad- and CuSNP-treated rat showing mild vacuolar degeneration associated with mildly congested blood vessels (H&E scale bar 20 µm).

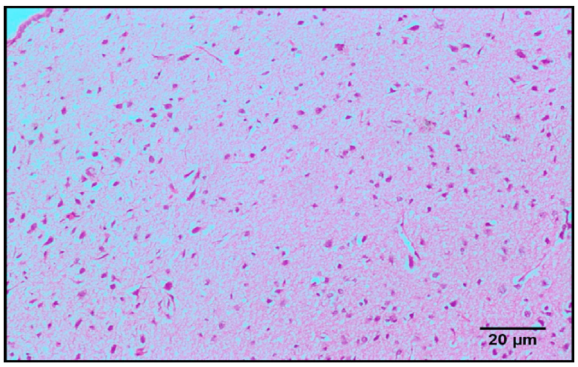

Figure 16. Photomicrograph of a section in the brain of a Cad + MSC-Exo + CuSNP-treated rat showing mild vacuolar degeneration (H&E scale bar 20 μm).

activity and improvement in the levels of ACh and AChT, which protect the neural cells from the toxic effects of Cad [44]. NPs may bind to AChE and affect the effectiveness of AChE after entering the body by spreading throughout the blood and the brain and primarily accumulating on the extracellular surface of erythrocytes and neurons [45].

Moreover, our results indicated that administration of Cad to normal rats resulted in a significant increase in the ROS levels, which is reflected in the significant reduction in the levels of TAC, compared with the normal rats. This may be attributable to the oxidative stress effect of Cad inducing the various pathological abnormalities similar to those observed in neurodegenerative diseases [46]. Consistent with our results, Ognjanovi'c et al. [47] found that Cad stimulates free radical production, resulting in the oxidative damage of lipids, proteins, and DNA. Parallel studies demonstrated that Cad is capable of increasing ROS indirectly by binding to functional protein groups. This disrupts the protein activity in the neural system, resulting in impaired TAC levels [48].

Our study demonstrated that treatment of rats with MSC-Exo, CuSNPs, or both resulted in a significant increase in the TAC levels, which is reflected in the significant reduction in the levels of ROS compared with the Cad group. Wang et al. [37] reported that MSC-Exo significantly inhibited ROS production and apoptosis in CSC subjected to oxidative stress injury. Exosomes act as a natural store for encapsulating bioactive molecules, such as proteins and RNA, to target them to the desired cells and to protect them from enzymatic degradation [49]. Along the same line, Guo et al. [50] found that the MSC-Exo elevated superoxide dismutase (SOD) levels and lowered the malondialdehyde (MDA), Lactate dehydrogenase (LDH), TNFα, and interleukin-1β (IL-1β) levels in the hippocampal neurons of rats with depression by upregulating the microRNA-26a expression.

CuSNPs enhanced the levels of TAC and strongly inhibited the levels of ROS, indicating that CuSNPs exert a neuroprotective effect against Cad toxicity. These results are consistent with prior reports, which revealed that NPs derived from metals are rich in antioxidants and may be used to eliminate free radicals [51]. Interestingly, it has been suggested that metal NPs have significant antioxidant activities, and they destroy numerous free radicals [52]. Moreover, our data agree with those of Zangeneh et al. [53], who established that CuNPs exhibit effective antioxidant properties owing to their benign and stable nature, non-cytotoxic effects, and antioxidant and antibacterial activities, indicating that they may be used as therapeutics.

Moreover, during the assessment of brain damage by Cad, the current data indicated that Cad administration produced a significant increase in the brain TNF-α and NF-κBlevels as compared with the Con group, whereas exposure to cadmium caused brain injury and dysfunction as a result of changes in the secretion of pro-inflammatory cytokines [54]. NF-κB is an inducible and inescapably pervasively expressed transcription factor for genes involved in various processes, including differentiation, cell survival, inflammation, and growth. This family of transcription factors is vital to the creation of inflammation. Distinct external stimuli can invigorate NF-κB, including carcinogens, tumor promoters, toxic metals, UV radiation, phorbol esters, asbestos, and alcohol [55] Critical cadmium exposure has been demonstrated to activate NF-κB in various systems. Furthermore, increased generation of ROS causes NF-κB to translocate from the cytoplasm to the nucleus, thus promoting the expression of various cytokines, including IL-1β and TNF-α [56].

Activated macrophages produce TNF-α, which magnifies and extends the inflammatory response and tissue injury by activating other cells that release cytokines, such as IL-1, and other mediators, such as nitric oxide and ROS [57]. Kundu et al. [58] investigated the effects of cadmium on the inflammatory response in the transformed A549 human lung adenocarcinoma epithelial cell line and found that Cad (2.5 μM) upregulated the expression of TNF-α at 24 and 48 h.

Treatment of Cad-intoxicated rats with MSC-Exo and CuSNPs or both showed a significant reduction in the brain NF-κB and TNF-α compared with the Cad group. MSC-Exo may improve neurological function by promoting tissue repair. Consistent with our results, Li et al. [59] found that treatment of experimental autoimmune encephalomyelitis (EAE) rats with MSC-Exo enhanced the TNF-α levels. This indicates that MSC-Exo modulates microglia polarization in theEAE models, which are considered as important immune cells in the CNS [60]. A parallel study demonstrated that MSC-Exocould insert bioactive tolerogenic molecules into auto-reactive lymphocytes and modify their phenotypes and promote the powerful ability of MSC-Exo to induce regulatory T cells [61]. Conversely, Zhang et al. [62] found that CuSNPs administered to animals with arthritis reduced pro-inflammatory modulator levels because of its anti-inflammatory effects. Moreover, CuSNPs destroyed various free radicals owing to their premium antioxidant activities [53]. Thus, the antioxidant and anti-inflammatory effects of MSC-Exo and CuSNPs may enhance the levels of NF-κB and TNF-α.

BDNF and NGF have been associated with the maturation, survival, and maintenance of neuron functions in the CNS [63], and their depletion leads to the development of neuronal injury and neurodegenerative diseases [64]. Our findings indicated a significant decrease in the brain BDNF and NGF levels after Cad exposure, which is in agreement with a previous report [65]. Liberation of BDNF and NGF depends on Cad displacing Ca^{2+} [66]. An excessive ROS production inhibits these neurotrophic proteins [67]. Therefore, antioxidant agents that target neurotrophic factors may protect the nervous tissue against Cad toxicity.

Treatment with MSC-Exo, CuSNPs, or in combination of both caused a significant increase in the BDNF and NGF levels in response to Cad exposure. Zhao et al. [68] demonstrated that BDNF is a direct target of miR-206. Consequently, the expression of BDNF was further amplified by miRNA knockdown. Studies demonstrated that exosomes contain miRNAs that can be transferred between cells and thus play a role in intercellular communication. Their role in neurodegeneration is an active area of investigation [69]. Moreover, MSC-Exoexerts an antioxidant effect through the inhibition of excessive ROS production stimulated by Cad exposure [70]. Furthermore, the ameliorative effect of CuSNPs on the restoration of BDNF and NGF levels may be attributed to different processes, including reduced ROS generation, oxidative damage repair, and enhanced antioxidative defense mechanisms [53]. Thus, the antioxidant effect of MSC-Exo and CuSNPs may participate in the amelioration of BDNF and NGF levels.

In the present study, we also examined the histology of rat brain tissues, which revealed that intervention withMSC-Exo and CuSNPs decreased the toxic effects of Cad on brain tissue. We also demonstrated the ability of MSC-Exo and CuSNPs to reduce degenerative changes that could result from neuronal disorders. Wolfe and Molinoff [71] suggested that brain degenerative changes could cause Alzheimer's disease in individuals exposed to Cad. Similarly, Sidman and Leviton [72] suggested that Cad may induce an untimely aging process. The discoveries from this study agree with those of Dzobo and Naik [73], who observed a lowering effect of selenium on cadmium-induced increases in esterase activity and oxidative stress in rat organs. This confirms the neuroprotective potential of MSC-Exo and CuSNPs and the safety of the doses administered in this

study. The possible mechanism of action of MSC-Exo and CuSNPs against cadmium-induced neurotoxicity may be involved in the regulation of cholinesterase activities, which attenuate antioxidant status, anti-inflammatory action, and nerve growth factors associated with neurological diseases.

Based on our results, we conclude that MSC-Exo and CuSNPs play a promising therapeutic role against Cad-induced neurotoxicity in male rats as evidenced by the improvements observed in behavioral and biochemical markers and confirmed by histological examination. These effects were achieved through the enhanced anti-cholinesterase, antioxidant, and anti-inflammatory properties of MSC-Exo and CuSNPs.Additional studies are needed to identify the specific proteins and other molecules transported by BMSC exosomes that contribute to microglia polarization, alleviation of inflammation, and tissue repair.

Declarations

Author contribution statement

Asmaa Magdy Zaazaa, Naglaa A. Ali, Safaa H Mohamed: Conceived and designed the experiments; Performed the experiments; Analyzed and interpreted the data; Contributed reagents, materials, analysis tools or data; Wrote the paper.

Bosy Azmy Abd El-Motelp, Ahmed M. Youssef, Mohamed Aly Sayed: Performed the experiments; Analyzed and interpreted the data; Contributed reagents, materials, analysis tools or data; Wrote the paper.

Funding statement

This research did not receive any specific grant from funding agencies in the public, commercial, or not-for-profit sectors.

Data availability statement

No data was used for the research described in the article.

Declaration of interests statement

The authors declare no conflict of interest.

Additional information

No additional information is available for this paper.

References

[1] L. Jarup, M. Berglund, C.G. Elinder, G. Nordberg, M. Vahter, Health effects of cadmium exposure-a review of the literature and risk estimate, Scand. J. Work. Environ. Health 24 (1998) 1–51. PMID: 9569444, www.ncbi.nlm.nih.gov/pubmed/9569444.

[2] P. Moyano, J.M. Garcíab, M. Loboa, M.J. Anadón, E. Solac, A. Pelayo, J. García, M.T. Frejo, J.D. Pino, Cadmium alters heat shock protein pathways in SN56 cholinergic neurons, leading to Aβ and phosphorylated Tau protein generation and cell death, Food Chemtox. 121 (2018) 297–308.

[3] O. Faroon, A. Ashizawa, S. Wright, P. Tucker, K. Jenkins, L. Ingerman, C. Rudisill, Toxicological Profile for Cadmium, ATSDR, Atlanta, GA, 2012.

[4] S. Jahan, A. Zahra, U. Irum, N. Iftikhar, H. Ullah, Protective effects of different antioxidants against cadmium induced oxidative damage in rat testis and prostate tissues, Syst. Biol. Reprod. Med. 60 (2014) 199–205.

[5] J.S. Heo, Y. Choi, H.S. Kim, H.O. Kim, Comparison of molecular profiles of human mesenchymal stem cells derived from bone marrow, umbilical cord blood, placenta and adipose tissue, Int. J. Mol. Med. 37 (1) (2016) 115–125.

[6] L.S. Sherman, A. Conde-Green, O.A. Sandiford, P. Rameshwar, Mesenchymal stromal/stem cells in drug therapy: new perspective, Cytotherapy 19 (1) (2017) 19–27.

[7] C.X. Li, N.P. Talele, S. Boo, A. Koehler, E. Knee-Walden, J.L. Balestrini, P. Speight, A. Kapus, B. Hinz, MicroRNA-21 preserves the fibrotic mechanical memory of mesenchymal stem cells, Nat. Mater. 16 (3) (2017) 379–389.

[8] Y. Yaghoubi, A.A. Movassaghpour, M. Zamanid, M. Mehdi Talebic, A. Mehdizadehf, M. Yousef, Human umbilical cord mesenchymal stem cells derived exosomes in diseases treatment, Life Sci. 233 (2019) 116733.

[9] J. Nicolas, S. Mura, D. Brambilla, N. Mackiewicz, P. Couvreur, Design and functionalization strategies for biodegradable/biocompatible polymer based nanoparticles applied in targeted drug delivery, Chem. Soc. Rev. 42 (2013) 1147–1235.

[10] A. Scharf, K.H. Gührs, A. von Mikecz, Anti-amyloid compounds protect from silica nanoparticle-induced neurotoxicity in the nematode C. Elegans, Nanotoxicology 10 (2016) 426–435.

[11] R. Uauy, M. Olivares, M. Gonzalez, Essentiality of copper in humans, Am. J. Clin. Nutr. 67 (1998) 952S–959S.

[12] N. Ramesh, M. Prasanth, T. Shanthini, K.M. Gothandam, S. Karthikeyan, B. Bozdogan, Nano-antibiotics, a therapeutic future, Nanosci. Nanotechnol. 7 (1) (2017) 3–25.

[13] M.T. Abdel Aziz, H.M. Atta, S. Mahfouz, H.H. Fouad, N.K. Roshdy, H.H. Ahmed, L.A. Rashed, D. Sabry, A.A. Hassouna, N.M. Hassan, Therapeutic potential of bone marrow derived mesenchymal stem cells on experimental liver fibrosis, Clin. Biochem. 40 (12) (2007) 893–899.

[14] N. Jaiswal, S. Haynesworth, A. Caplan, S. Bruder, Osteogenic differentiation of purified, culture-expanded human mesenchymal stem cells in vitro, J. Cell. Biochem. 64 (1997) 295–312.

[15] C. Bang, S. Batkai, S. Dangwal, S.K. Gupta, A. Foinquinos, A. Holzmann, A. Just, J. Remke, K. Zimmer, A. Zeug, E. Ponimaskin, A. Schmiedl, X. Yin, M. Mayr, R. Halder, A. Fischer, S. Engelhardt, Y. Wei, A. Schober, T. Thum, Cardiac fibroblast-derived microRNA passenger strand-enriched exosomes mediate cardiomyocyte hypertrophy, J. Clin. Invest. 124 (5) (2014) 2136–2146.

[16] T.T.Q. Hoa, L.V. Vu, T.D. Canh, N.N. Long, Preparation of ZnS nanoparticles by hydrothermal method, J. Phys. Conf. 187 (2009), 012081.

[17] D. Mohamed, A. Saber, A. Omar, A. Soliman, Effect of cadmium on the testes of adult albino rats and the ameliorating effect of zinc and vitamin E, Br. J. Sci. 11 (1) (2014) 72–95. Corpus ID: 43676253.

[18] W. Nassar, M. El-Ansary, D. Sabry, M.A. Mostafa, M. Temraz, E.K. Saad, A.N. Saad, W. Essa, H. Adel, Umbilical cord mesenchymal stem cells derived extracellular vesicles can safely ameliorate the progression of chronic kidney diseases, Biomater. Res. 5 (2016) 21.

[19] E. Cholewińska, K. Ognik, B. Fotschki, Z. Zduńczyk, J. Juśkiewicz, Comparison of the effect of dietary copper nanoparticles and one copper (II) salt on the copper biodistribution and gastrointestinal and hepatic morphology and function in a rat model, PLoS One 13 (5) (2018), e0197083.

[20] Wills D. DesikanA, C. Ehlers, Ontogeny and adolescent alcohol exposure in Wistar rats: open field conflict, light/dark box and forced swim test, PharmacolBiochemBehav 122 (2014) 279–285.

[21] S. Tsakiris, K.H. Schulpis, K. Marinou, P. Behrakis, Protective effect of L- cysteine and glutathione on the modulated suckling rat brain Na+,K+-ATPase and Mg2+-ATPase activities induced by the in vitro galactosaemia, Pharmacol. Res. 49 (2004) 475–479.

[22] O.H. Lowry, N.J. Rosebrough, A.L. Farr, R.J. Randall, Protein measurement with the folin phenol reagent, J. Biol. Chem. 193 (1951) 265–275.

[23] C. Oswald, S.H. Smits, M. Hoing, L. Sohn-Bosser, L. Dupont, D. Le Rudulier, L. Schmitt, E. Bremer, Crystal structures of choline/acetylcholine substrate-binding protein chox from sinorhizobiummeliloti in the liganded and unligznded-closed states, J. Biol. Chem. 283 (2008) 32848–32859.

[24] R.J. Henry, Principles and Tech, Harper u. Row Publishers Inc. Clin Chem. II Edition, 1974, p. 917. https://www.worldcat.org/title/clinical-chemistry-principles-and-technics/oclc/216650549?referer=di&ht=edition.

[25] D.G. Koracevic, G. Koracevic, V. Djordjevic, S. Andrejevic, V. Cosic, Method for the measurement of antioxidant activity in human fluids, J. ClinPathol. 54 (2001) 356–361.

[26] J. Adams, Proteasome inhibition in cancer development of PS-341, Semin. Oncol. 28 (6) (2001) 613–619.

[27] D. Intiso, M.M. Zarrelli, G. Lagioia, F.D. Rienzo, C.D. Ambrosio, P. Simone, P. Tonali, R.P. Cioffi, Tumor necrosis factor alpha serum levels and inflammatory response in acute ischemic stroke patients, Neurol. Sci. 24 (2004) 390–396.

[28] Y.A. Barde, The nerve growth factor family, Prog. Growth Factor Res. 2 (1990) 237–248.

[29] J.D. Banchroft, A. Stevens, D.R. Turner, Theory and Practice of Histological Techniques, fourth ed., Churchil Livingstone, New York, London, San Francisco, Tokyo, 1996.

[30] M.D. Abramoff, P.J. Magelhaes, S.J. Ram, Image processing with image, J. Biophotonics. Inter. 11 (7) (2004) 36–42. www.researchgate.net/publication/228334776.

[31] P. Armitage, G. Berry, Comparison of several groups, in: Statistical Method in Medical Research, second ed., Blockwell significant publication, Oxford, 1987, pp. 186–213.

[32] C. Dhandapani, R. Narayanasamy, S.N. Karthick, H. Kuzhandaivel, Dr, S. Samayanan, P. Hemalatha, M. kumar, K. Selvaraj, Hee-Je Kim, Drastic photocatalytic degradation of methylene blue dye by neodymium doped zirconium oxide as photocatalyst under visible light irradiation, Optik - Int. J. Light Elec. Opt. (2016) 127.

[33] A. Phuruangrat, T. Thongtem, S. Thongtem, Characterization of copper sulfide hexananoplates, and nanoparticles synthesized by a so no chemical method, Chalcogenide Lett. 8 (4) (2011) 291–295. https://chalcogen.ro/291_Phuruangrat.pdf.

[34] S.H. Ma, L.L. Zhang, Q.Q. Jiang, Protective effect of bioflavonoid morin on cadmium induced oxidative, Neuropathology 28 (2017) 1148–1154.

[35] H.X. Geng, L. Wang, Cadmium: toxic effects on placental and embryonic development, Environ. Toxicol. Pharmacol. 67 (2019) 102–107.

[36] M. Kippler, F. Tofail, J.D. Hamadani, R.M. Gardner, S.M. Grantham-McGregor, M. Bottai, M. Vahter, Early-life cadmium exposure and child development in 5-year-old girls and boys: a cohort study in rural Bangladesh, Environ. Health Perspect. 120 (10) (2012) 1462–1468.
[37] Y. Wang, R. Zhao, D. Liu, W. Deng, G. Xu, W. Liu, J. Rong, X. Long, J. Ge, B. Shi, Exosomes derived from miR-214-enriched bone marrow-derived mesenchymal stem cells regulate oxidative damage in cardiac stem cells by targeting CaMKII, Aug 7;2018, Oxid. Med. Cell. Longev. (2018) 4971261.
[38] B. Mead, S. Tomarev, Bone marrow-derived mesenchymal stem cells-derived exosomes promote survival of retinal ganglion cells through miRNA-dependent mechanisms, Stem Cells Transl. Med. 6 (4) (2017) 1273–1285.
[39] F. Zeng, Y. Wu, X. Li, X. Ge, Q. Guo, X. Lou, C. Zhonglian, H. Bingwen, N.J. Long, Y. Mao, Custom-made ceria nanoparticles show a neuroprotective effect by modulating phenotypic polarization of the microglia, Angew. Chem. 130 (2018) 5910–5914.
[40] K. Jomova, M. Valko, Advances in metal-induced oxidative stress and human disease, Toxicology 283 (2011) 65e87.
[41] M. Mendez-Armenta, C. Rios, Cadmium neurotoxicity, Environ. Toxicol. Pharmacol. 23 (3) (2007) 350–358.
[42] M.J. Glat, D. Offen, Cell and gene therapy in Alzheimer's disease, Stem Cell. Dev. 22 (10) (2013) 1490–1496.
[43] J.S. Snyder, Questioning human neurogenesis, Nature 555 (7696) (2018) 315–316.
[44] Z. Wang, J. Zhao, F. Li, D. Gao, B. Xing, Adsorption and inhibition of acetylcholinesterase by different nanoparticles, Chemosphere 77 (1) (2009) 67–73.
[45] M. Stasiuk, D. Bartosiewicz, A. Kozubek, Inhibitory effect of some natural and semisynthetic phenolic lipids upon acetylcholinesterase activity, Food Chem. 108 (2008) 996–1001.
[46] S.K. Agnihotri, U. Agrawal, I. Ghosh, Brain most susceptible to cadmium induced oxidative stress in mice, J. Trace Elem. Med. Biol. 30 (2015) 184–193.
[47] B.I. Ognjanovic, S.D. Markovic, N.Z. Ethordevic, I.S. Trbojevic, A.S. Stajn, Z.S. Saici ́c, Cadmium induced lipid peroxidation and changes in antioxidant defense system in the rat testes: protective role of coenzymeQ10andvitaminE, Reprod. Toxicol. 29 (2) (2010) 191–197.
[48] C.T. Aiken, R.M. Kaake, X. Wang, L. Huang, Oxidative stress-mediated regulation of proteasome complexes, Mol. Cell. Proteomics 10 (5) (2011) 1–11.
[49] A. Akbari, N. Jabbari, R. Sharifi, M. Ahmadi, A. Vahhabi, S.J. Seyedzadeh, M. Nawaz, S. Szafert, M. Mahmoodi, E. Jabbari, R. Asghari, J. Rezai, Free and hydrogel encapsulated exosome-based therapies in regenerative medicine, Life Sci. 249 (2020) 117447.
[50] H. Guo, B. Huang, Y. Wang, Y. Zhang, Q. Ma, Y. YumingRen, Bone marrow mesenchymal stem cells-derived exosomes improve injury of hippocampal neurons in rats with depression by upregulating microRNA26a expression, Int. Immunopharm. (82) (2020) 106285.
[51] M. Hamelian, M.M. Zangeneh, A. Amisama, K. Varmira, H. Veisi, Green synthesis of silver nanoparticles using Thymus kotschyanus extract and evaluation of their antioxidant, antibacterial and cytotoxic effects, Appl. Organomet. Chem. 32 (2018) e4458.
[52] V. Ball, Polydopaminenanomaterials: recent advances in synthesis methods and applications, Front. Bioeng. Biotechnol. 17 (2018) 109.
[53] M.M. Zangeneh, H. Ghaneialvar, M. Akbaribazm, M. Ghanimatdan, N. Abbasi, S. Goorani, E. Pirabbasi, A. Zangene, Novel synthesis of Falcaria vulgaris leaf extract conjugated copper nanoparticles with potent cytotoxicity, antioxidant, antifungal, antibacterial, and cutaneous wound healing activities under in vitro and in vivo condition, J. Photochem. Photobiol., B: Biology 197 (2019) 1–13, 111556.
[54] H.S. Alnahdi, I.A. Sharaf, Possible prophylactic effect of omega-3 fatty acids on cadmium-induced neurotoxicity in rats' brains, Environ. Sci. Pollut. Res. 26 (2019) 31254–31262.
[55] M. Valko, H. Morris, M.T.D. Cronin, Metals, toxicity and oxidative stress, Curr. Med. Chem. 12 (2005) 1161–1208.
[56] R.S. Almeer, R.B. Kassab, G.I. AlBasher, A. Alarifi, S. Alkahtani, D. Ali, A.E. Abdel Moneim, Royal jelly mitigates cadmium-induced neuronal damage in mouse cortex, Mol. Biol. Rep. 46 (1) (2019) 119–131.
[57] K.J. Tracey, The inflammatory reflex, Nature 420 (2002) 853–859.
[58] S. Kundu, S. Sengupta, A. Bhattacharyya, EGFR upregulates inflammatory and proliferative responses in human lung adenocarcinoma cell line (A549), induced by lower dose of cadmium chloride, Inhal. Toxicol. 23 (2011) 339–348.
[59] Z. Li, F. Liu, X. He, X. Yang, F. Shan, J. Feng, Exosomes derived from mesenchymal stem cells attenuate inflammation and demyelination of the central nervous system in EAE rats by regulating the polarization of microglia, Int. Immunopharm. 67 (2019) 268–280.
[60] V.E. Miron, A. Boyd, J.W. Zhao, T.J. Yuen, J.M. Ruckh, J.L. Shadrach, et al., M2 microglia and macrophages drive oligodendrocyte differentiation during CNS remyelination, Nat. Neurosci. 16 (2013) 1211–1218.
[61] A. Mokarizadeh, N. Delirezh, A. Morshedi, G. Mosayebi, A.A. Farshid, B. Dalir-Naghadeh, Phenotypic modulation of auto-reactive cells by insertion of tolerogenic molecules via MSC-derived exosomes, Vet. Res. Forum 3 (2012) 257–261.
[62] Z. Zhang, A. Chinnathambi, S.A. Alharbi, L. Bai, Copper oxide nanoparticles from Rabdosiarubescens attenuates the complete Freund's adjuvant (CFA) induced rheumatoid arthritis in rats via suppressing the inflammatory proteins COX-2/PGE2, Arab. J. Chem. 13 (6) (2020) 5639–5650.
[63] T. Numakawa, H. Odaka, N. Adachi, Actions of brain-derived neurotrophin factor in the neurogenesis and neuronal function, and its involvement in the pathophysiology of brain diseases, Int. J. Mol. Sci. 19 (11) (2018) 3650.
[64] M.S. Abdelfattah, S.E.A. Badr, S.A. Lotfy, G.H. Attia, A.M. Aref, A.E. Abdel Moneim, R.B. Kassab, Rutin and selenium co-administration reverse 3- nitropropionic acid-induced neurochemical and molecular impairments in a mouse model of Huntington's disease, Neurotox. Res. 37 (2020) 77–92.
[65] H.R. Marini, D. Puzzolo, A. Micali, E.B. Adamo, N. Irrera, A. Pisani, G. Pallio, V. Trichilo, C. Malta, A. Bitto, F. Squadrito, D. Altavilla, Neuroprotective effects of polydeoxyribonucleotide in a murine model of cadmium toxicity, Oxid. Med. Cell. Longev. 2018 (2018) 4285694.
[66] M.O. Kadry, R.A. Megeed, Probiotics as a complementary therapy in the model of cadmium chloride toxicity: crosstalk of beta-catenin, BDNF, and STAR signaling pathways, Biol. Trace Elem. Res. 185 (2) (2018) 404–413.
[67] G. Hacioglu, A. Senturk, I. Ince, AlverA, Assessment of oxidative stress parameters of brain-derived neurotrophic factor heterozygous mice in acute stress model, Iran J. Basic Med. Sci. 19 (4) (2016) 388–393.
[68] H. Zhao, Y. Li, L. Chen, C. Shen, Z. Xiao, R. Xu, J. Wang, Y. Luo, HucMSCs-derived miR-206-knockdown exosomes contribute to neuroprotection in subarachnoid hemorrhage induced early brain injury by targeting BDNF, Neuroscience 417 (2019) 11–23.
[69] H. Xin, Y. Li, B. Buller, M. Katakowski, Y. Zhang, X. Wang, X. Shang, Z.G. Zhang, M. Chopp, Exosome-mediated transfer of miR133b from multipotent mesenchymal stromal cells to neural cells contributes to neurite outgrowth, Stem Cell. 30 (2012) 1556–1564.
[70] S.U. Kim, Y.H. Park, Y.S. Min, H.N. Sun, Y.H. Han, J.M. Hua, T.H. Lee, S.R. Lee, K.T. Chang, S.W. Kang, J.M. Kim, D.Y. Yu, S.H. Lee, D.S. Lee, Peroxiredoxin I is a ROS/p38 MAPK-dependent inducible antioxidant that regulates NF-kappaB-mediated iNOS induction and microglial activation, J. Neuroimmunol. 259 (1–2) (2013) 26–36.
[71] B.R. Wolfe, P.B. Molinoff, Heavy metal toxicity in the 21 st century, Toxicology 85 (2012) 125–129.
[72] J.B. Sidman, A.M. Leviton, Effects of cadmium exposure on the physiology of neuron, Eng J. Med. 356 (2005) 98–107.
[73] K. Dzobo, Y.S. Naik, Effect of selenium on cadmium-induced oxidative stress and esterase activity in rat organs, South Afr. J. Sci. 109 (5/6) (2013) 965.